ROLE OF 2-DEOXY-D-GLUCOSE IN INDUCING AUTOPHAGY IN CANCER CELLS

By: Juliet Nana Esi Baidoo
E-mail: Juliet.Baidoo@csi.cuny.edu
Home Institution: The Graduate Center, City University of New York (CUNY)
Summer Research Principal Supervisor: Dr. Juliane Bogner-Strauss
E-mail: Juliane.Bogner-Strauss@tugraz.at
Summer Research Institution:
Graz University of Technology (TU Graz), Graz - Austria
Duration of Research: August – October 2017
Scholarship: The Marshall Plan Foundation
Sponsoring Program:
New York City Louis Stokes Alliance for Minority Participation (NYC-LSAMP)

ROLE OF 2-DEOXY-D-GLUCOSE IN INDUCING AUTOPHAGY IN CANCER CELLS

By: Juliet Nana Esi Baidoo
Principal Supervisor: Dr. Juliane Bogner-Strauss
2017 Summer Research: Marshall Plan Scholarship

ABSTRACT

Autophagy is activated during stressful and nutrient deprived conditions in the cellular environment. This process helps to provide an alternative source of nutrient for the cell by breaking down amino acids and other nutrients. 2-deoxyglucose is known to inhibit glycolysis, therefore initiating autophagy. We therefore hypothesized that treating cells with 2-deoxyglucose will activate autophagy in cancer cells, whereas supplying the cells with an alternate energy source; N-acetyl-aspartate, would suppress this effect.

Significance: In understanding the mode by which cancer cells provide themselves with alternate sources of nutrients for growth and metastasis, a better perspective of finding a treatment can be generated to help curb this overbearing pandemic.

INTRODUCTION

Lung cancer is one of the leading causes of cancer deaths in the United States (US) as well as the world in general. This project focuses on the role of glucose deprivation in inhibiting cancer cell growth. Several biochemical and environmental factors influence tumor growth and metastasis. In this experiment, we planned on investigating the role that 2-deoxy-glucose, a glycolysis inhibitor, plays in regulating autophagy in LLC1 (Lewis lung carcinoma) cells. Before we delve into the summer project, lets first learn a bit about the major aspects of this project: autophagy, 2-deoxy-glucose, N-acetyl aspartate (NAA), and Lung cancer.

Autophagy

Autophagy is derived from the Greek words *auto* which means "self" and *phagein* meaning "to eat"; therefore the literal translation of autophagy is "self-eating". It refers to the degradation of cytoplasmic components within the lysosome [Zannotto-Filno et al., 2014]. The word was first coined by Christian de Duve about four decades ago when he used it to describe the degradation of the mitochondria and other intra-cellular structures within the lysosome of a rat liver perfused with glucacon [Yang & Klionsky, 2009]. In eukaryotic cells, there are three major types of autophagy: macroautophagy, microautophagy, and chaperone-mediated autophagy. All three types a mechanistically different from each other. Micro- and macroautophagy involves membrane rearrangement to engulf portions of the cytoplasm with a capacity of sequestering large structures like organelles. However, microautophagy deals with the direct engulfment of the cytoplasmic contents at the lysosome through invagination, protrusion, and septation of the lysosome membrane, while in macroautophagy portions of the cytoplasm are sequestered into the de novo formed double-membrane vesicle known as autophagosome. This eventually leads to the fusion of the autophagosome with the lysosome and consequent release of inner single-membrane vesicles into the lumen to be further broken down and transported as macromolecules back into the cytosol through membrane permeases for reuse [Yang and Klionsky, 2009]. Chaperone-mediated autophagy on the other hand involves the translocation of unfolded soluble proteins directly across the lysosome; it therefore serves as a transport system for proteins, which would have otherwise not been able to cross the limited-membrane of the lysosome [Yang and Klionsky, 2009]. Macroautophagy (hereafter referred to as autophagy) has several physiological roles. It aids in the removal of damaged organelles and the recycling of long-lived proteins. It is a coping mechanism for cells during stressful conditions such as nutrient deprivation, heat and oxidative stress. It is also involved in cellular development and differentiation, and is implicated in a lot of diseases such as cancer, Alzheimer's disease, Parkinson's disease, Huntington's disease, and Crohn's disease, among others [Levine, 2007; Levine and Klionsky, 2004; Glick et al. 2010]. Biochemical pathways and proteins that regulate autophagy are the mechanistic target of rapamycin (mTOR), Ras/PKA (protein kinase A), AMPK (adenosyl monophosphate kinase), Atg9, Atg8, Atg5, Atg7, Atg10,

Atg12, LC3, PE (phosphatidylethanolamine), PI3K (phosphatidylinositol 3-kinase), [Yang and Kilionsky, 2009; Levine and Klionsky, 2004; Levine and Kroemer, 2008].

In the absence of a tumor, autophagy is known to suppress tumor formation, however, in the presence of tumor, it promotes tumor growth by providing it with nutrients while inhibiting pathways that are responsible for curbing tumor growth [Galluzzi et al., 2017]. Autophagy is therefore referred to as a double-edged sword in tumorigenesis and metastasis [Zhu and Bu, 2017]. It is however unclear as to whether activating or inhibiting autophagy is effective in potentiating the chemotherapeutic response of some cancer-targeted drugs. Galluzzi et al. analyzed these two effects on cancer drugs on autophagy and concluded that chemotherapeutic drugs are more effective if they activate autophagy instead of inhibiting it [Galluzi et al., 2017]. One major marker of autophagy is the microtubule-associated proteins 1A/1B light chain 3B (MAP1LC3B or LC3) protein, which is highly expressed in the presence of autophagy, as autophagosomal compartments increase in size. Stressful cellular conditions repress the activity of mTOR which is responsible for regulating cellular growth and metabolism. This triggers the formation of matured and isolated autophagosomes upon the conversion of LC3 to LC3I (via the removal of C-terminal 22 amino acid from LC3) and the further conversion of some LC3I to LC3II (a lipid-modified form of LC3) hence making this protein a very important marker for autophagy [Zhu and Bu, 2017; Zannotto-Filno et al., 2014]. The exact role that LC3 protein plays in autophagy is still under investigation by research scientists.

2-Deoxy-Glucose (2-DG)

Glycolysis is the metabolic pathway that converts glucose to pyruvate. 2-deoxyglucose is a glucose molecule in which the 2-hydroxyl group is replaced by hydrogen [Sun at al., 2010]. During the process of glycolysis, this 2-hydroxyl group on glucose is phosphorylated by hexokinase to form glucose-6-phosphate (G6P) which further goes through the glycolytic pathway to produce energy in the form of ATP (adenosine triphosphate) for cellular growth and survival. In the absence of the 2-hydroxyl group (forming the 2-deoxy-glucose, 2-DG), the

phosphorylation reaction is unable to take place, hence preventing the glucose molecule from undergoing glycolysis [Korcok et al., 2003]. 2-DG is a good marker for the detection of diseases such as cardiovascular diseases, tumors, and Alzheimer's disease. It is able to achieve this purpose when it is radiolabelled with fluorine-18 (fluorodeoxyglucose, FDG), and used to check for glucose metabolism using a positron emission tomography (PET) scan. This scan shows increased glucose uptake in tumor tissues compared to the normal ones [Stein et al., 2010]. While normal cells produce energy through oxidative phosphorylation, cancer cells rely on glycolysis and lactic acid fermentation to produce ATP in high oxygen conditions. This process is known as the Warburg Effect [Vander et al., 2009]. In tumors, 2-DG is taken up by glucose transporters and competes with glucose for phosphoglucoisomerase binding during the second step of glycolysis. This slows down the rate of glycolysis, and through this mechanism, has been shown to subsequently inhibit growth of various tumor types *in vitro* and *in vivo* [Seo et al., 2014]. 2-DG is currently under investigation as an anticancer and antiviral agent [Korcok et al., 2003].

N-acetyl aspartate (NAA)

N-acetyl aspartate is found in exceptionally high levels in the central nervous system (CNS). It is actually the second largest metabolite in the brain, with glutamate being the first [Ariyannur et al., 2010; Moffet et al., 2007]. In 2007, Moffet and company, explained that the concentration of NAA can be as high as 10 mM or even more. Due to its high presence in the brain, NAA has proven to be a very reliable marker for understanding the brain's functionality using magnetic resonance spectroscopy (MRS) [Moffet et al., 2007; Moffett et al., 2013]. This provides a better way of diagnosing certain brain disorders as an excessive increase or drastic decrease in NAA levels could be a signal for an onset of certain brain disorders. For instance, NAA has been associated with Canavan disease. This disease results from a mutation in the gene encoding for the enzyme aspartoacyclase (ASPA) which is responsible for the breakdown of NAA. This mutation results in the buildup of NAA, a leading cause of progressive infantile leukodystrophies, an example of which is Canavan disease [Hoshino and Kubota, 2014].

Therefore there is a correlation between NAA levels in the brain and neuronal health and integrity [Hoshino and Kubota, 2014]. Diseases that can be detected with changes in NAA levels via MRS are brain cancer (decreased NAA), multiple sclerosis (decreased NAA), epilepsy (decreased NAA), Alzheimer's disease (decreased NAA) and Canavan disease (increase in NAA), among others [Moffet et al., 2007; Moffett et al., 2013].

NAA is synthesized from a reaction between acetyl-CoA and aspartate. This reaction is catalyzed by the enzyme Nat8l (N-acetyltransferase 8-like). In oligodendrocytes, NAA plays a role in myelination and myelin repair [Ariyannur et al., 2010]. Additionally, Ariyannur et al. has proposed that since NAA is synthesized using acetyl-CoA in the brain, it may serve as a storage and transport system for the *de novo* synthesis of acetyl–CoA in oligodendrocytes, following its breakdown by ASPA and acetyl-CoA synthase-1/2 (AceCS1/2) [Ariyannur et al., 2010].

NAA also plays a role in lipid synthesis, protein and histone acetylation (via AceCS1 in the cytoplasm and nucleus), and energy derivation via the TCA cycle (via AceCS2 in the mitochondria) and elevated NAA levels in lung and ovarian cancer results in worse patient outcome [Pessentheiner et al., 2013; Prokesch et al., 2016; Zand et al., 2016]. Consequently, we predict that NAA might be a significant source of energy for growing tumors [Pessentheiner et al., 2013; Prokesch et al., 2016; Zand et al., 2016]. Likewise, understanding the mechanisms underlying the energy derivation ability of NAA in cancer will help in formulating therapeutic drugs for cases when prognosis is poor, such as late-stage lung cancer diagnosis.

Lung Cancer

Cancer cells grow uncontrollably and overcrowd normal cells. Some cancer cells may start in the lung and grow in the bone. This does not make it a bone cancer but instead a lung cancer as it originates from the lung. This process of cancer cells moving to and growing in different parts of the body is known as metastasis. When cancer develops in a tissue or organ and forms a lump, it is becomes a tumor. Cancerous lumps are referred to as malignant tumors while non-cancerous lumps are benign tumors.

This paper will focus on lung cancer.

Lung cancers usually start developing in the cells lining the bronchi and parts of the lung such as the bronchioles and alveoli. There are three types of lung cancer, non-small cell lung cancer (85% of lung cancers), small cell lung cancer (10-15% of lung cancers), and lung carcinoid tumor (5% of lung cancers). Small cell and non-small cell lung cancers are the second most common type of cancer with the first being prostate cancer (for men) and breast cancer (for women) [Travis et al., 2011]. Lung cancer is the leading cause of cancer death compared to breast, prostate, and colon cancers. Women are more likely to get diagnosed with lung cancer than women with the ratio being 1 in 17 to 1 in 15 for women and men respectively. These ratios increase with smoking. Also, black men are 20% more likely to develop lung cancers than white men and its diagnosis is usually common in older individuals of 65 years or older with a few cases seen in people younger than 45 years old. Due to its late stage diagnosis, this cancer becomes almost impossible to treat. Consequently, only 7% of lung cancer patients survive for at least five years after diagnosis [National Cancer Institute, 2017].

Lewis lung carcinoma (LLC1) cells produce tumors in mice that are relatively less hemorrhagic, and therefore have a semi-firm tumor mass. This cell line is also known for its high tumorigenic and low metastatic properties in mice. According to a report by cancer chemotherapy from 1972, LLC1 cells are very useful in studying the metastasis of cancer in mice and developing drug targets. Since cancer cells are known to rely on aerobic glycolysis for ATP production, a process that is termed the Warburg effect [Sun et al., 2017], it is safe to say that a process that inhibits glycolysis could serve as a source of hindering cancer cell or tumor growth. In this study, we have investigated the efficacy of 2-deoxyglucose (2-DG) in inducing autophagy in LLC1 cells. If this is indeed the case, we predict that NAA treatment in these cells would prevent or suppress an autophagy response induced by 2-DG, since it provides an alternate route for energy metabolism. Therefore, we measured LC3 expression, as an indicator of autophagy, in both Nat8l overexpressed (Nat8l o/e) versus control (PuroN1) LLC1 cells. We hope that this study will serve as a foundation for further mechanistic studies in understanding the role of

cancer drugs in autophagy, and how targeting this process, can be effective strategy in the elimination of cancer cells.

METHODS:

Retroviral Expression of Nat8l in Monoclonal Cell Lines

Full-length coding sequence of murine *Nat8l* was amplified by PCR from murine adipose tissue cDNA using *Phusion* polymerase (Fermentas) and cloned into a murine stem cell virus vector (pMSCV puro, BD Biosciences Clontech) using the restriction sites XhoI/EcoRI. To produce infectious but replication-incompetent recombinant retroviruses expressing *Nat8l*, PhoenixEco packaging cells (cultured in DMEM with 10% FBS in 5% CO_2) were transfected with pMSCV-*Nat8l* using Metafectene (Biontex Laboratories GmbH). The supernatant containing the viral particles was collected 48 h after transfection. Viral supernatants were supplemented with 8 µg/ml Polybrene and added to LLC1 cells (30–40% confluence) for infections for 18–24 h. Because cells could not be selected with puromycin, single cells were picked under the microscope and expanded as monoclonal populations, and overexpression was controlled by quantitative RT-PCR. Differentiation was induced as described above. As a control for the above described stable cell lines, the empty pMSCVpuro was used and underwent the same procedure (Pessentheiner et al. 2013).

Cell Culture

Puro-N1 and Nat8l overexpressed (Nat8l o/e) Lewis Lung Carcinoma (LLC1) cells were cultured in DMEM medium until they reached about 60% confluency. At this point, the cells were seeded in two ways, one for mRNA expression and the other for protein estimation to further be used for western blotting analysis. For these purposes, 60,000 and 30,000 cells were seeded into a 6-well plate for protein studies and RNA studies, respectively. First the cells were observed under the microscope to ensure that they are not too confluent as they start differentiating upon reaching confluency and we wanted to avoid this since our test was for a proliferation assay. Prior to starting the seeding process, a water bath is turned on and set to

37°C. Upon reaching the set temperature, a bottle of trypsin and DMEM medium (without pyruvate) containing pen-strep antibiotic and 10% FBS (fetal bovine serum) is put into the water bath to warm up. This is important as it ensures that the medium and trypsin are at the same temperature as the cellular conditions in the incubator. Without taking this precaution, you stand the risk of stressing the cells and this could lead to cell death due to the drastic change in temperature -- 37°C for the cells in the flask from the incubator to 4°C of the medium and trypsin. Upon reaching the desired temperature (about 15 to 30 minutes), the bottles and/or falcon tubes are wiped dry, alcohol-sprayed, and transferred into an alcohol-cleaned biosafety cabinet with a blower on to help maintain sterility of the cells and the work environment. Also, alcohol-spray serological pipets and falcon tubes before keeping in the biosafety cabinet for use during the seeding process. Label the falcon tubes with respect to the corresponding cells in the T-75 flask that you intend to put into them. For instance, PuroN1 and Nat8l o/e cells for each tube. With all your working materials ready, transfer your cells-containing T-75 flasks from the incubator into the biosafety cabinet. Now you are ready to begin the seeding process.

First, aspirate the medium from the cells in the flask and add about 5 ml of sterile phosphate buffer saline (PBS) to wash the cells. This ensures the removal of dead cells and serum-containing DMEM medium as the presence of FBS will slow down the activity of the trypsin. Add 2 mL of trypsin to the cells – this aids in the detachment of the adherent cells from the bottom of the plate. Gently bang the sides of the flask in your palm and then transfer it unto a heating plate (set at 37°C) for about 2 minutes. Observe the plate under a microscope to ensure the complete or almost complete removal of cells from the bottom of the plate, which is indicated by the floating of the cells in he trypsin. Then transfer the flask back into the biosafety cabinet and neutralize the trypsin with medium of a volume that is 4 times the volume of trypsin (8 mL of serum-containing DMEM). Using a serological pipet, ensure that the trypsin and medium are uniformly mixed and that there are almost no cells still attached to the flask. Then transfer the entire contents of the flask into a falcon tube. Repeat the above steps for remaining flasks. Then centrifuge the falcon tube for 5 minutes at 1200 rpm. After centrifugation, wipe tubes clean with alcohol and transfer back to the biosafety cabinet. Aspirate the supernatant (containing the medium and trypsin), leaving behind the pellet, which

are your cells. Resuspend the cells in 2 mL of serum-containing medium and transfer 10 uL onto a hmeacytometer for counting. Using a cell counter, count the cells. You will get a value in cells per mL; for instance, 2.56 x 10^5 cells/mL. Multiply this number by 2 (the total volume of your cell suspension) to get 512,000 cells in 2 mL cell suspension. This is the total number of cells you got from your just-trypsinized T-75 flask. To seed say 30,000 cells into three wells of a 6-well plate, each cell will hold a volume of 2 mL. So you multiply the 3 wells by 2 mL to get 6 mL total volume for all three wells with 30,000 cells per well (90, 000 wells in the 6 mL total volume). To find out how much volume to pick up from the 2 mL cell suspension to make a volume of 6 mL cell suspension of 90, 000 cells, first multiply the 90,000 cells by 2 mL and divide the product by 512,000 cells to get 0.3515 mL. This means, you will pick up about 352 µL of the 2 mL cell suspension and make up the volume to 6 mL. Then, from this 6 mL, you pick up and distribute 2 mL per well of the 6-well plate. This gives you 30,000 cells per well for the mRNA expression assay. Repeat the above for the remaining cells as well as for the protein assay plates of 60,000 cells per well. Label plates with name of cells, passage number, number of cells, date and your initials. Observe plate under the microscope to ensure even distribution cells in the well and incubate at 37°C 5% CO_2 incubator.

Treatment with 2-deoxyglucose (2-DG)

After 24 hours of seeding, the cells were treated with 2mM 2-DG and 0.1mM 2-DG. 1 M 2-DG was incubated in the 37°C water bath prior to treatment. To treat the cells with a concentration of 2 mM and 0.1 mM 2-DG in 2 mL, we added 4 uL and 0.2 uL respectively to the wells. Then DMEM wells (without any 2-DG treatment) served as control for the treatment while the LLC1 PuroN1 cells served as a control for the LLC1 Nat8l o/e cells.

Treatment with NAA

After 24 hours of seeding, the cells were treated with 10mM NAA. 100 mM NAA was incubated in the 37°C water bath prior to treatment. To treat the cells with a concentration of 10 mM NAA in 2 mL, we added 200 uL of the 100 mM NAA to the wells. DMEM wells served as a control for the treatment while the LLC1 PuroN1 cells served as a control for the LLC1 Nat8l o/e cells. Both

NAA and 2mM 2-DG were used to treat cells within the same well to investigate the effect of simultaneous administration.

Western Blot

24 hours following treatment, the cells were washed with 1X PBS and harvested on ice by adding 100 µL of SDS lysis buffer containing protease inhibitor cocktail, shaking for about 5-10 minutes (in a cold room) and scraping of the cells with a cell scraper. Transfer cells into a 1.5mL microcentrifuge tube. Incubate lysate at 95°C for 5 minutes. Add 0.3 µL of nuclease and incubate at room temperature for 35 minutes. Centrifuge for 3 minutes at 15.000 g. Transfer supernatant into a newly labeled tube and store on ice. Perform BCA Assay using the Pierce™ BCA Protein Assay Kit to estimate the amount of protein in each vial. Using the results from the assay, 30µg of protein were loaded onto a 4-12% premade gel which was run using either MOPS or MES buffer for 65 minutes at 165 V. The gel was transferred unto a PVDF membrane using 1X TGS buffer for 90 minutes in a cold room. To view the completion of transfer and the presence of proteins, the membrane was stained with Ponceau S stain for 15 minutes, washed with PBST and imaged using a Syngene Imager. The blots were then blocked for 1 hour at room temperature in 5% milk buffer or 1% BSA – 5% milk buffer for β-actin and LC3 detection, respectively. Blots were incubated in primary antibodies (LC3 1:1000, rabbit; and β-actin 1:25000, mouse) overnight at 4°C while shaking. After incubation with primary antibody, the blots were washed three times with PBST and incubated with secondary antibody (α-rabbit 1:5000; α-mouse 1:3000) for 2 hours at room temperature while shaking. Blots were washed with PBST three times for 10 minutes per wash, and incubated in 1:1 ratio of ECL detection reagents for 5 minutes and then imaged using Syngene Imager to observe the LC3 and beta-actin protein expressions as shown by the dark bands with respect to the molecular weight of the proteins (LC3I = 19kDa, LC3II = 17kDa, and β-actin = 42 kDa).

mRNA Expressions

24 hours following treatment (of the 30,000 cells per well of the 6-well plate), the cells were washed with 1X PBS and harvested on ice by adding 500 µL of RNA lysis buffer from the ExtractMe RNA isolation kit. Following the protocol in the kit, RNA was extracted from the

harvested cells and cDNA content was accounted for. qPCR analysis was run on the cDNA samples to test for relative mRNA expression of various genes.

Quantitative Real Time PCR (qPCR)

RNA isolation and reverse transcription were performed as described above. RT-PCR analysis was performed in 96-well plates in a total volume of 4 µl containing 2 ng of original total RNA using the QuantiFast SYBR Green RT-PCR kit (Qiagen, Germany) and validated QuantiTec primer assays (Qiagen, Germany) according to the manufacturer's instructions for Light Cycler 480 instruments. In brief, after the initial 5-min heat activation step at 95 °C, cycling conditions were as follows: 40 cycles of denaturation at 95 °C for 10 s, combined annealing and extension at 60 °C for 30 s. The PCR efficiency of the target and housekeeping genes was determined by cDNA dilution series prepared from an untreated sample. Results were corrected with the LightCycler relative quantification software (Roche Diagnostics).

Data Analysis

Western blot bands were quantified using Image J and the data were analyzed using Graph Pad Prism or Microsoft Office Excel. Data from the qPCR were also quantified using Graph Pad Prism.

Assisted another Ph.D. student in performing mouse surgery

Upon my arrival in Dr. Bogner-Strauss's laboratory, I was asked to give a brief talk on my research at the City University of New York's College of Staten Island (CUNY, CSI).

My research focuses on finding an alternative treatment for Glioblastoma and other forms of cancers that is void of the deleterious side effects that the current treatment with chemotherapy and radiotherapy are associated with. In so doing, we use a compound known as curcumin, derived from the turmeric plant which is used as a food spice in south-east Asia. During my research, I intracranially implant GL261 glioblastoma cancer cells into the mice, allow the tumor to be established (~ 8 to 11 days), treat mice intraperitoneally with curcumin and curcumin-phytosome (a lipid-encapsulated form of curcumin; day 12 to day 42 or more), then

sacrifice the mice and extract the brains for immunohistochemistry, flow cytometry, and other forms of tests.

With this knowledge, the lab kept in mind that I had some expertise in brain extractions among other things. As a result, when one of the graduate students (Gabriel) needed help with extracting organs from insulin-treated mice for further analysis, they asked if I could help and I was more than excited to do so as I had missed working with mice.

Prior to the surgery, each mouse was weighed and injected with insulin and its blood was tested (time 0). Then this testing was done at different time points, say 5, 10, 15, 30, and 60 minutes and the values were recorded. Immediately following the last test, the mouse was anesthetized and prepared for surgery. Gabriel extracted the white adipose tissues, liver, kidneys, spleen, brown adipose tissues, and muscular tissues from the thighs. Then he transferred the mouse to me to extract the brain. In extracting the brain, I first decapitated the mouse and used surgical scissors to de-skin the head to expose the skull. Then, using a micro scissors, I made an incision in the skull and gently peeled it off to expose the brain. This step has to be done with extra care to prevent rapturing the brain. The brain was carefully scooped up and transferred to a small petri dish. The brain and other organs were immediately washed with phosphate buffer saline (PBS), weighed, and transferred to a micro-centrifuge tube. This tube was then placed in a tank containing liquid nitrogen for snap-freezing. We extracted organs from a total of eight mice. The micro-centrifuge tubes containing the various tissues were later transferred into -80°C freezer for long-term storage.

Kathy, the graduate student I worked with directly, and Gabriel, used this as an opportunity to learn how to extract brain as I explained the process to them during the extraction and answered every question they had regarding the process. After extracting seven brains, I asked Kathy to extract the last brain with my guidance. Excited to not only learn, but also do something new (she worked with cells for the most part), she followed my instructions and carefully extracted the eighth brain.

This was one of the highlights of my research in the Bogner-Strauss laboratory as I learned how to extract other tissues and organs from the mice, extracted mouse brains, and successfully taught some students (Kathy and Gabriel) how to extract brain from the mouse.

RESULTS AND DISCUSSION

In a preliminary experiment at the Bogner-Strauss Lab, LLC1 PuroN1 cells (control) and Nat8l o/e (experimental) cells were cultured in the presence and absence of pyruvate, glutamine and glucose to test for cell proliferation in these environments. The result from this assay showed that both PuroN1 and Nat8l o/e cells relied on glutamine for their survival. Glucose deprivation resulted in a decreased cell proliferation in the PuroN1 cells; however, Nat8l o/e cells coped better without glucose, presumably because they are better equipped to rely on NAA as an alternate source of energy. Both cell groups did not show any differential effect with or without pyruvate. Following these findings, all cell culture experiments were done in a pyruvate-free medium containing glucose and glutamine. A treatment with NAA cells showed an increase in PuroN1 cells but had no effect on Nat8l o/e cells. The major difference in proliferation was seen at 2mM 2-DG and 10mM NAA concentrations (Data not shown). Consequently, we settled with these two concentrations for the autophagy experiments.

Relative mRNA expression

A qPCR analysis was performed to investigate the expression of various autophagy markers in the presence of a nutrient-deprived environment (2mM 2-DG) compared to control (DMEM). The results showed that the LC3II mRNA was highly expressed in the presence of 2mM 2-DG treatment in both the PuroN1 cells as well as the Nat8l o/e cells; however, the mLC3b (LC3II mRNA) levels was slightly higher in the PuroN1 cells compared to the Nat8l o/e cells (Figure 1). Other autophagic mRNA's were also highly expressed in a likely manner, such as mLamp1, and mLamp2.

A

Sample Name	36b4 r+f	mLC3a	mLC3b	mLamp1	mLamp2
LLC1 puroN1 A DMEM	18.47364616	28.5207634	24.17767525	22.3727169	23.86148453
LLC1 puroN1 B DMEM	17.99429321	27.64470863	23.99069023	21.65710258	23.87220955
LLC1 puroN1 C DMEM	17.78032303	28.04804611	23.77232742	21.51344681	23.58280182
LLC1 Nat8l1 O/E A DMEM	17.81382751	28.12675285	23.70106888	21.51652718	23.75545883
LLC1 Nat8l1 O/E B DMEM	17.68161392	27.77375221	23.75819778	21.24251366	23.51198006
LLC1 Nat8l1 O/E C DMEM	17.53277016	27.97538185	23.70348167	21.65659714	23.64230537
LLC1 puroN1 A 2mM 2DG	18.79862022	28.33145332	23.87155724	21.95462608	23.01714325
LLC1 puroN1 B 2mM 2DG	19.15293121	29.46273422	23.99727249	21.93198013	23.17592812
LLC1 puroN1 C 2mM 2DG	18.94199181	28.62268448	24.01220894	21.67724037	23.10657692
LLC1 Nat8l1 O/E A 2mM 2DG	17.97973633	28.21807671	23.52492523	21.37420273	23.05840302
LLC1 Nat8l1 O/E B 2mM 2DG	17.91052628	28.22767639	23.4567337	20.39971161	23.23841667
LLC1 Nat8l1 O/E C 2mM 2DG	18.53010941	28.70255661	23.72685242	21.92545509	23.5093956
LLC1 puroN1 A 0.1mM 2DG	18.74006844	28.9356575	24.61661911	21.88339996	23.73771095
LLC1 puroN1 B 0.1mM 2DG	18.90822792	28.98552704	24.92607117	22.52626038	23.9807148
LLC1 puroN1 C 0.1mM 2DG	18.05000305	28.46875	24.16420937	21.92717361	23.89644432
LLC1 Nat8l1 O/E A 0.1mM 2DG	17.84497261	28.25888443	24.00185966	21.37458611	23.46723938
LLC1 Nat8l1 O/E B 0.1mM 2DG	18.01754379	28.25598907	23.97546387	21.76576233	23.90007973
LLC1 Nat8l1 O/E C 0.1mM 2DG	17.92328644	28.10756111	23.97226715	21.73991203	23.91247559

B

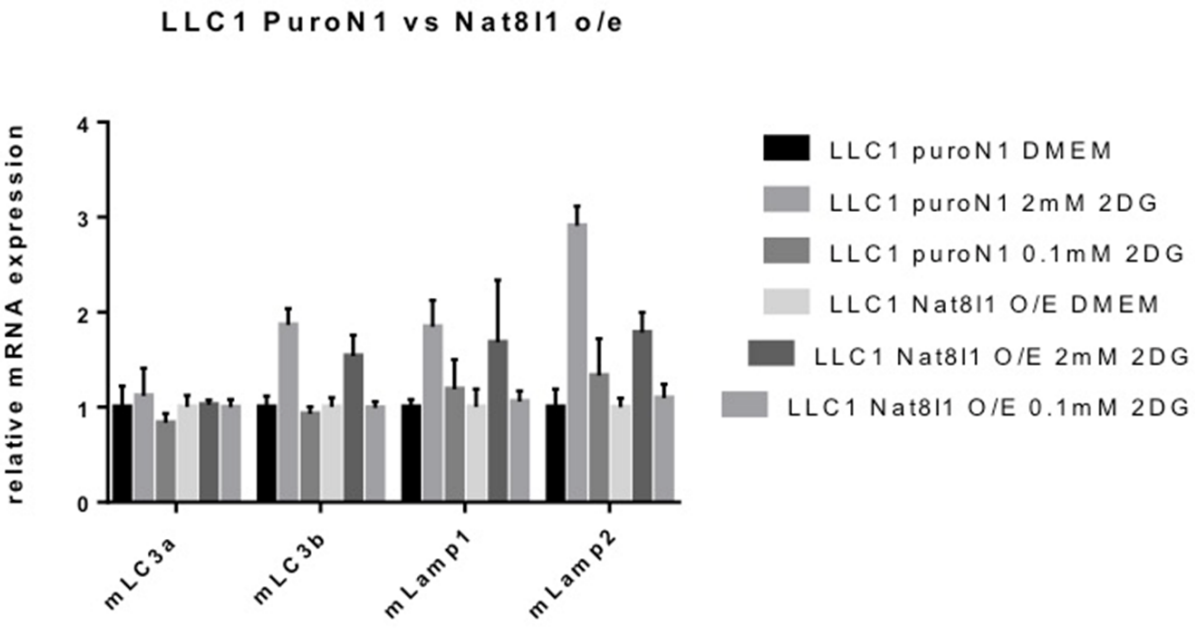

Figure 1: qPCR analysis shows the expression of LC3a and b mRNA as well as Lamp1 and 2 mRNA. (A) is a table showing the C_T values from the qPCR analysis. (B) shows an increase in relative mRNA expression of LC3a and b in Nat8l o/e LLC1 cells compared to PuroN1.

MOPS or MES Buffer Running Buffer?

60,000 LLC1 cells were seeded in 6-well plates, then treated with 2mM 2-DG, 0.1mM 2-DG and DMEM (control). These cells were harvested after 24 hours of treatment with lysis buffer and a western blotting analysis was conducted using MOPS running buffer in one experiment, and MES running buffer in another (Figures 2A and B respectively). The results showed that the MOPS running buffer was a better choice for running the SDS-Page gel electrophoresis as it gave a much better and more crisp separation of the LC3I (Top) & LC3II (bottom) bands. Although the MES buffer also gave a good separation, the bands seemed a bit smudged. Based on these results, we proceeded with running the subsequent gels with MOPS running buffer.

A

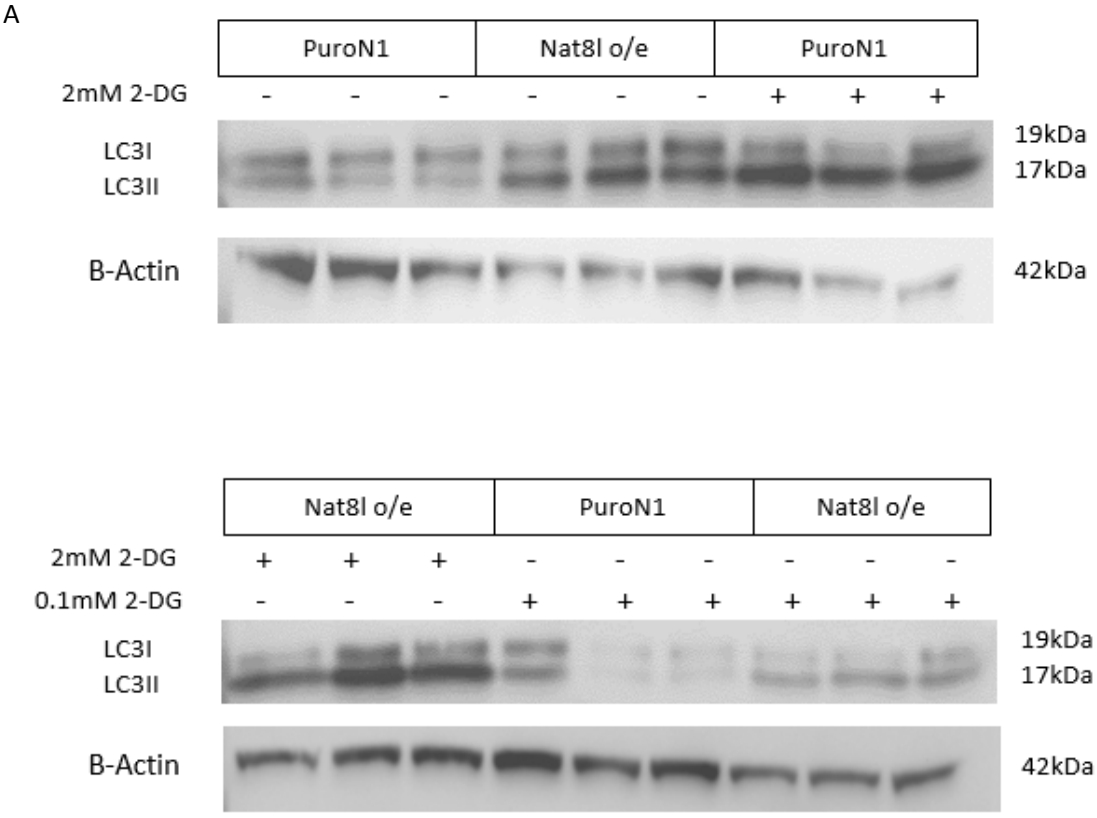

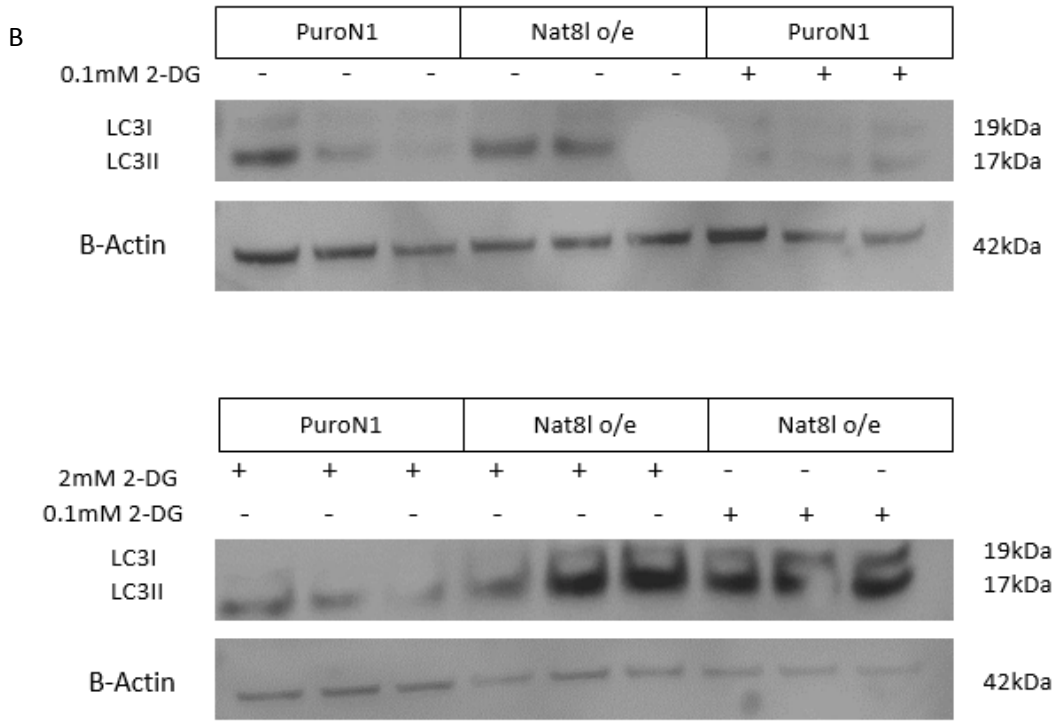

Figure 2: Both MOPS (A) and MES (B) buffers show a high expression of LC3 in Nat8l o/e cells, and less in PuroN1, relative to the loading control B-actin.

All treatment groups on one gel help give a better comparison between groups.

Knowing what buffer to use, we ran another set of gels with three different biological replicates of the PuroN1 and Nat8l o/e cells, given the same treatment as described above in Figures 2 A and B. Each treatment group was assigned to each gel and a comparison was made between the PuroN1 groups and the Nat8l o/e groups. However, since all the three treatment groups were found on different gels, we could not make a good comparison between the individual treatment groups (control, 2mM 2-DG, and 0.1mM 2-DG). Despite our inability to accurately compare the effect of 2-DG treatment on the LLC1 cells, we saw that the 2mM 2-DG-treated cells, showed an increase in LC3II expression compared to the DMEM and 0.1mM 2-DG groups. Also, the DMEM and 0.1mM 2-DG-treated groups did not show any significant difference (Figure 3). Quantifying these data with Image J showed that there was a significant decrease in

LC3II protein expression in Nat8l o/e cells in both the control and 2mM 2-DG groups. No major difference was seen between the different biological replicates (Figure 3 lanes 1, 2, & 3).

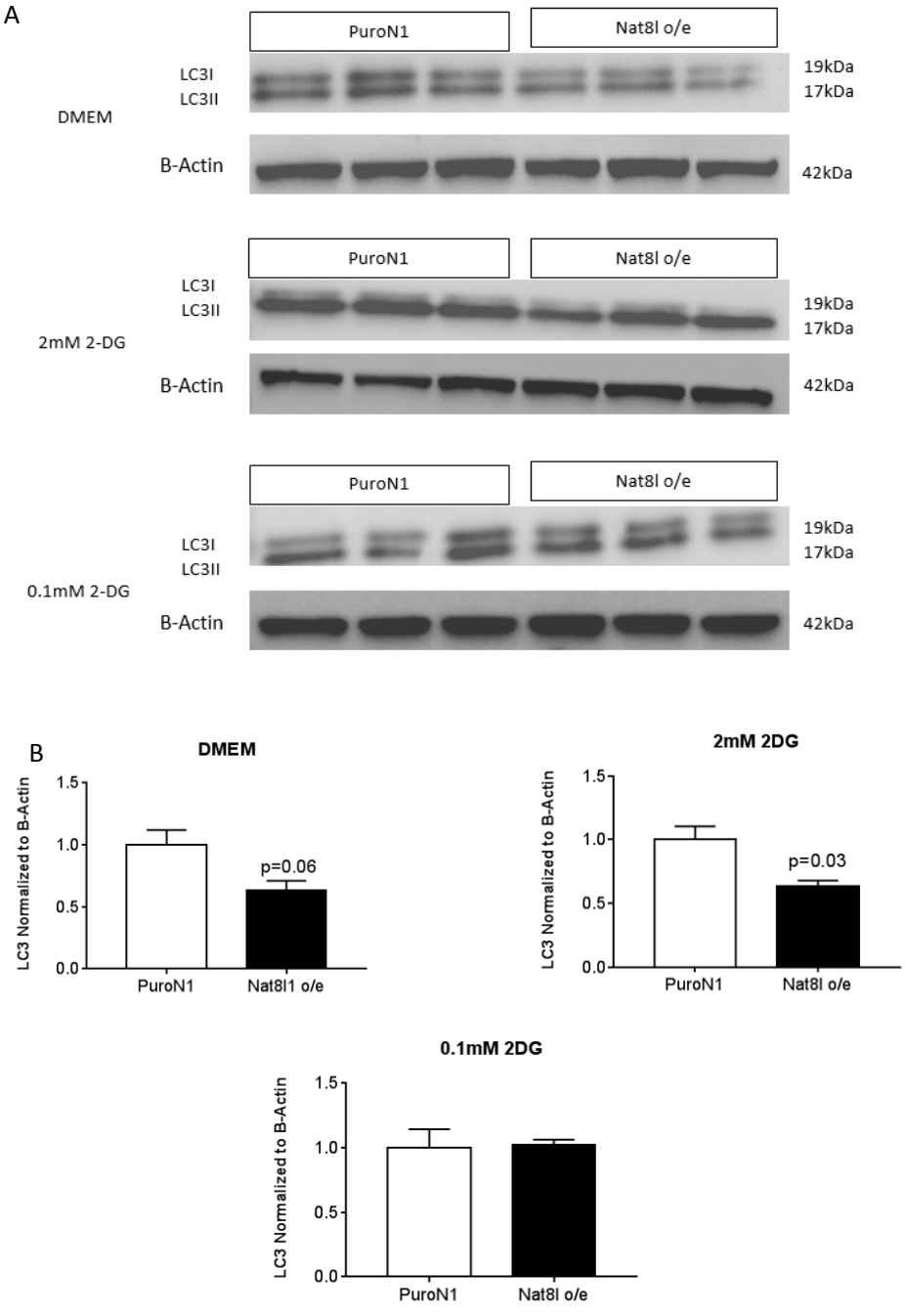

Figure 3: Running three gels to represent the three treatment groups, makes it difficult to compare and analyze the data across groups. Western blots (A) showing a decrease in LC3 protein in Nat8l o/e cells compared to PuroN1 (B). Not much difference was observed between the DMEM and 2mM 2-DG treatment groups. The 0.1mM 2-DG group showed same results for PuroN1 and Nat8l o/e.

10% Gel obscures the expression of the LC3 protein

In correcting our setback from the previous western blot experiment, we ran the next western blot with all of the three treatment groups on one gel (Figure 4). This blot showed that while there was a low expression of LC3II in the control (DMEM), the 2mM 2-DG group showed an increase in expression of LC3II protein. To replicate the above data, another gel was run. This time, we used a 10% gel instead of the 4-12% gel. This data (Figure 5) gave the same result as seen in Figure 4 where LC3II expression was elevated following 2mM 2-DG treatment. The problem with this gel, however, was that the LC3 protein was detected as one solid band. It is important to see two bands for the expression of the LC3 protein, as LC3I is converted into LC3II with the onset of autophagy. Therefore, one solid band is not representative of the data. We concluded from these two experiments that the 4-12% gel is better for the expression of LC3 protein as it shows both the LC3I and the LC3II bands. We re-probed the 10% gel with the Nat8l antibody to verify that the Nat8l protein was still present in our cells. As shown in Figure 5A & C, there was no Nat8l expression in the PuroN1 cells, as indicated by the lack of bands in lanes 1, 3, and 5. The Nat8l o/e cells showed bands for Nat8l protein expression, which decreased upon treatment with 2mM and 0.1 mM 2-DG as seen in lanes 2, 4, and 6 (Figure. 5A & C). A quantification of this data showed that treatment with 2mM 2-DG increased the expression of LC3 protein in the PuroN1 cells (Figure 5B & D).

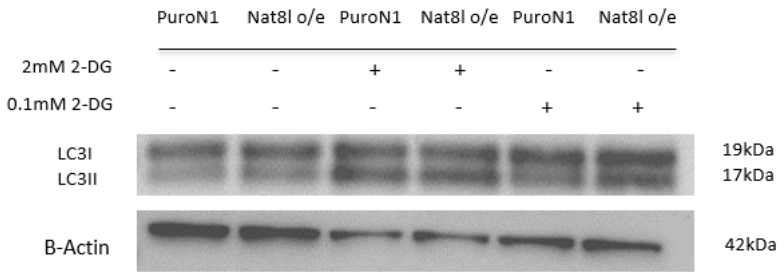

Figure 4: Western Blot bands show a high expression of LC3 protein with 2mM 2-DG treatment.

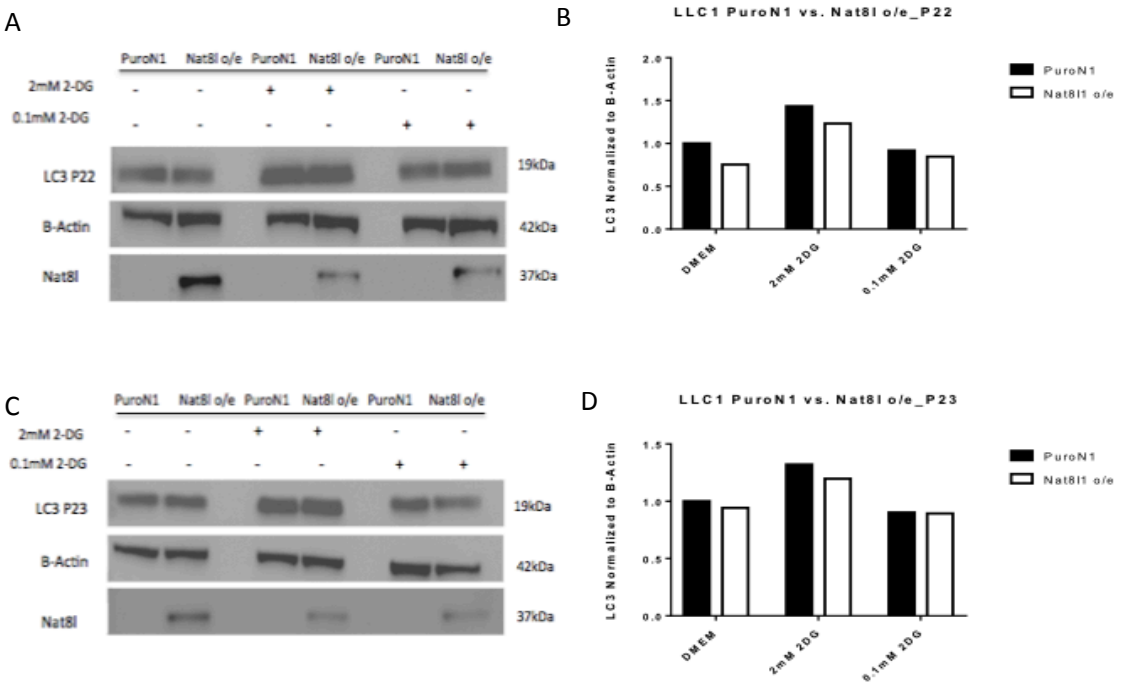

Figure 5: Running the samples on 10% gel gives inseparable bands for LC3 protein (A & C). Treatment with 2mM 2-DG provides an increase in both PuroN1 and Nat8l o/e LC3 expression (B & D). Nat8l protein is present and decreases in expression with 2-DG treatment. P22 & P23 are two biological replicates of the LLC1 PuroN1 and Nat8l o/e cells.

2-DG Induces Autophagy?

Upon establishing the need for 4-12% gel for optimal detection of the LC3I and LC3II proteins, we replicated the results from Figure 5 using a MES instead of a MOPS buffer. Although we had concluded from Figure 2, that MOPS buffer was a better option for running the gels, we needed to validate this claim in another experiment, as one gel does not give a good basis for drawing such solid conclusion. As shown in Figure 6, we notice that the bands are very comparable to that of the MOPS bands (Figure 4); however, the bands seemed slightly curved on the ends when MES buffer was used to run the gels. It is important to note that while the bands may look different, the overall data is same in both the MOPS and MES buffer, where LC3 bands were lowly expressed in the DMEM and 0.1mM groups while highly expressed in the 2mM 2-DG-treated group. In furtherance of the above, the onset of autophagy is made evident in the bands of the LC3 protein expression: in the DMEM bands, we see a higher expression of LC3I compared to LC3II protein, but the reverse of this observation is seen in the 2mM 2-DG treated bands. This throws more light on the induction of autophagy, which is activated by the treatment with 2mM 2-DG; hence the formation of autophagosomes was made evident by the low expression of LC3II in DMEM (Figure 6A lanes 1 & 2 for both P19 & P23) but high in 2mM 2-DG treatment (Figure 6A lanes 3 & 4 for both P19 & P23). Once again, there was not much variance seen across different biological replicates (P19 and P23). It is also important to note that in this figure, within biological replicates, there is a great increase in LC3II expression in the Nat8l o/e groups compared to the PuroN1 groups. There is also an increase in LC3II expression in PuroN1 groups across the two biological replicates; nonetheless, this increase is more pronounced in the P19 group than in the P23 group (Figure 6B). These differences tell us that the same drug could have different effects on different individuals, given their varying physiological conditions.

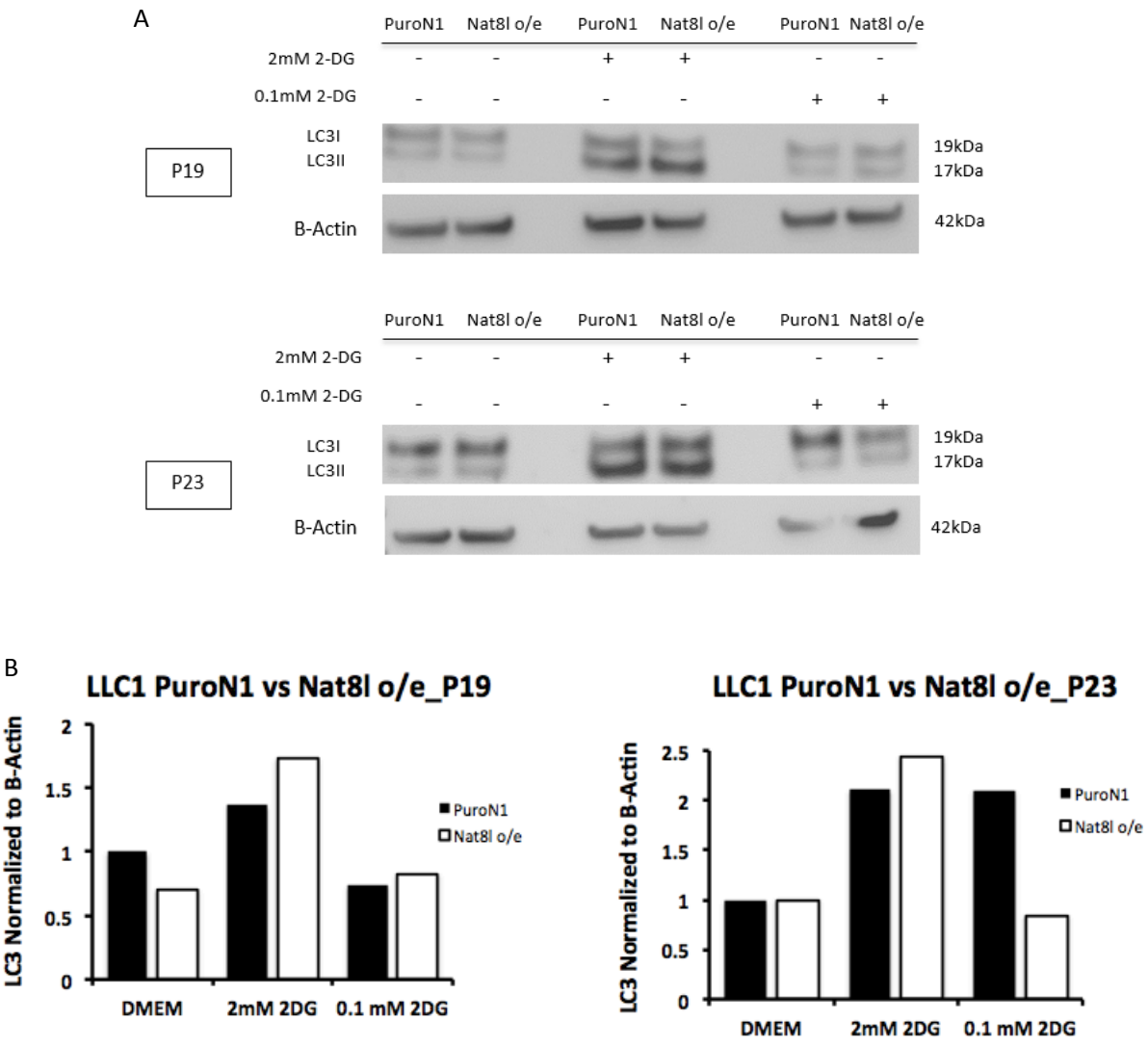

Figure 6: ***Treatment of LLC1 cells with 2mM 2-DG increases LC3 expression in both PuroN1 and Nat8l o/e cells.*** Here we observe an increase in LC3II expression (A) with 2mM 2-DG treatment in both PuroN1 and Nat8l o/e cells, as well as their different biological replicates (P19 -Top & P23 - Bottom blot). Although there is an increase in both PuroN1 and Nat8l o/e expression of LC3II protein, the increase in the Nat8l o/e cells is much more pronounced (that is more than twice of the control) (B) than it is in the PuroN1 cells.

Treatment with NAA restores the cells to their normal condition

Now that we have evidence that 2mM 2-DG indeed induces autophagy, we went on to investigate the role of NAA in the treatment of the LLC1 cells. In Figure 7A, we show that while LC3II is highly expressed in the presence of 2mM 2-DG treatment (Lanes 3 & 4), NAA treatment decreases the expression of LC3 protein (Lanes 7 & 8). More importantly, when both drugs were combined in treatment, the result was similar to that of the 2-DG-only treatment, except the expression was much higher (Figure 7B). There is therefore an inverse relationship between the effects of 2mM 2-DG and that of 10mM NAA on LLC1 cells, as one increases LC3 expression while the other decreases its expression. NAA is known to provide an alternative source of nutrition by catabolizing into acetate and aspartate by ASPA, and then further being converted to acetyl CoA by the enzyme acetyl CoA synthetase1 and 2. This newly formed acetyl CoA is recruited by the citric acid cycle to produce energy. Aspartate is also used as a source of oxaloacetate and other metabolites in the body. This explains the increase in Nat8l o/e in the 10mM NAA-treated cells.

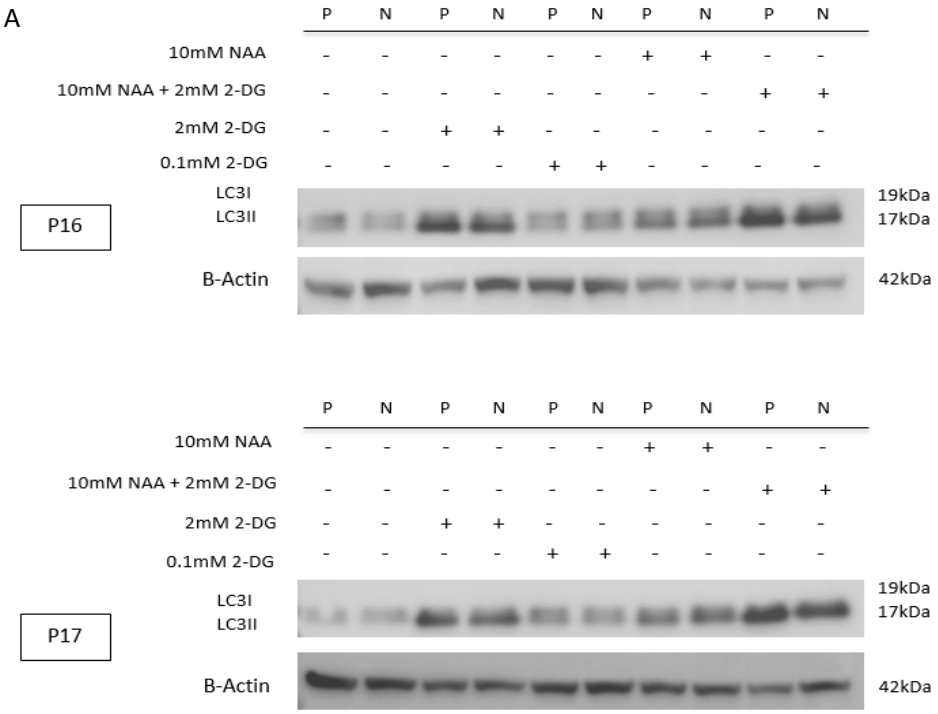

B

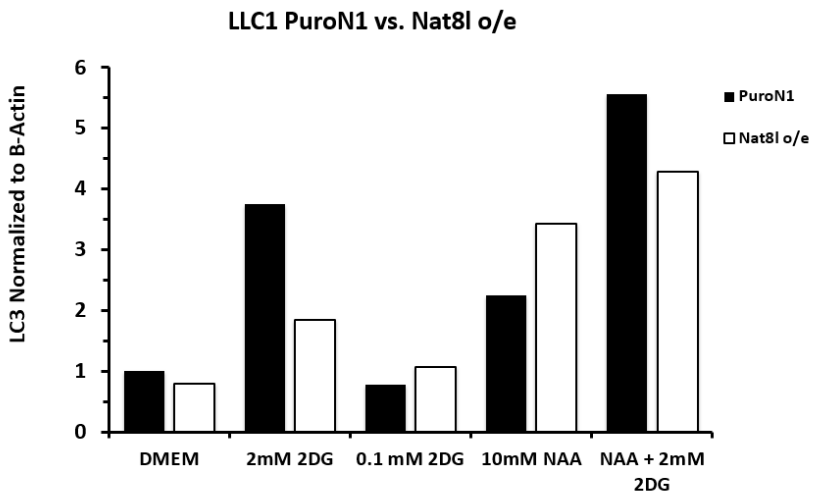

Figure 7: Treatment of LLC1 cells with NAA reverses the effect of 2mM 2-DG. We see an increase in LC3 expression with 2mM 2-DG treatment as well as 2mM 2-DG + 10 mM NAA treatment (A) in both biological replicates (P16 -Top & p17-Bottom blot). Although there is an increase in both PuroN1 and Nat8l o/e expression of LC3 protein, the increase in the PuroN1 is much more pronounced than it is in the Nat8l o/e. Inversely, comparing 2mM 2-DG with 10mM NAA treatment results in a decrease in PuroN1 but an increase in Nat8l o/e LC3 expression.

Different Biological replicates yield varying results

All experiments were performed on different biological replicates of the cell (example: P22, P23, P16, P19, etc). Intriguingly, we observed a difference across biological replicates: in some cases, we saw an increase in autophagy with 2mM 2-DG treatment, while in other cases, 2mM 2-DG treatment resulted in a decrease in autophagy. These differences were observed throughout the experiments. A possible source of error could have been the difference in person's handling the cells. Although the same cellular conditions were maintained throughout the experiment, the cell culture was done by two different people. Each person (myself and the graduate students whose project I was working on) may have used slightly different methods of culturing, treating, or harvesting the cells. While this is not a major source of error or differences in results, it is important to note that a small change of hands, could result in a slight change of conditions which in turn might help or hurt the cells. For instance,

Based on these differences in results, it is very difficult to draw a conclusion that the 2mM 2-DG treatment promotes the activation of autophagy. We would first have to standardize this experiment by using one biological replicate.

CONCLUSION

In these experiments, we compared the effect of 2mM 2-DG and NAA treatment on LLC1 cells. Nat8l is the enzyme responsible for the synthesis of NAA; therefore, under nutrient-deprived conditions the expression of this protein should be low. As shown in Figures 2 and 4, there is greater expression of LC3II in the Nat8l o/e group with 2-DG treatment; however, the reverse of this is seen in Figure 3. Also, in Figures 5, 6, and 7, the control and experimental cell lines of the LLC1 cell (PuroN1 and Nat8l o/e) show an increase in LC3II expression when treated with 2mM 2-DG. It is important to note that this increase varies across experiments. In Figure 6, the LC3II expression in Nat8l o/e cells increases to greater the twice the control. Then, in Figure 7, we see the same increase for Nat8l o/e as in Figure 6, but the PuroN1 increased to about three times the control - showing a much greater expression of LC3II in the PuroN1 than in the Nat8l o/e cells. Comparing the NAA with the 2mM 2-DG treatment groups, we see an approximately two-fold increase in the Nat8l o/e cells while the PuroN1 LC3II expression was decreased to about half of the control. Finally, combining both 2mM 2-DG and 10mM NAA in treatment also gave an increase in both PuroN1 and Nat8l o/e expression LC3II protein in a much greater capacity than observed in the control.

From our results, we observed that a treatment with 2mM 2-DG, which creates a nutrient-deprived environment, leads to both an increase and decrease in Nat8l o/e LLC1 cells. Due to the varying results across biological replicates and across experiments, it is difficult to draw a decent conclusion regarding the effect of 2mM 2-DG on LLC1 cells. While we can confidently say that 2mM 2-DG is inducing autophagy from the increase in LC3II expression with 2-DG treatment, it is uncertain as to how this works. That is, is it Nat8l overexpression-dependent or not? This question remains unanswered from these experiments. As a result, further work is required to elucidate this problem.

Additional investigation that explores the mechanisms involved in autophagosomal production is vital in the development of effective therapeutics for cancer treatment.

FUTURE WORK

Besides the increase in LC3II protein expression levels, little is known about the mechanisms involved in the activation of autophagy by treatment with 2-DG. It is essential to investigate the effect of 2-DG on autophagic pathways such as mTOR, Bcl2, and Bax, as they will throw more light on and help provide a much deeper understanding of the role of autophagy in cancer cell growth and metastasis.

In a recent publication, Mukherjee et al. showed that curcumin phytosome has effective anticancer properties as well as immunotherapeutic effects in repolarizing the brain's immune system from M2 (immunosuppressive and tumor promoting) microglia to the M1 (antitumor) phenotype [Mukherjee et al., 2016]. Curcumin is a compound in the turmeric plant that gives it its yellow color. It is known to be responsible for the low rate of colon cancer in the south east Asian countries and has been implicated in numerous types of cancers due to its anticancer and anti-inflammatory properties. One of its well-known modes of mechanism in controlling or treating tumor growth is via its ability to inhibit the tumor-promoting protein Nf-κB while activating the cell cycle inhibiting protein, P53. Despite its promising effects, curcumin is insoluble in water and has a low bioavailability, hence limiting its ability to become a highly potent and dependable cancer treatment agent [Langone et al. 2014]. Curcumin phytosome (Meriva®) is a lipid-encapsulated form of curcumin which is soluble in water and has a higher bioavailability as compared to curcumin. Mukherjee and his colleagues investigated the role of curcumin phytosome in treating glioblastoma brain cancer in mice and found that curcumin phytosome does not only help to prolong the survival rate of glioblastoma-tumor mice, but also repolarized the macrophages of the tumor microenvironment from the M2 tumor-promoting phenotype to the M1 tumor suppressing phenotype [Mukherjee et al. 2016]. Now 2-DG is also known to play a certain role in the repolarization of the M2 to M1 microglia and is more effective when combined with other cancer treatment agents; however this role and its

mechanism is still under investigation [Zhao et al., 2017]. It will therefore be insightful to investigate the role of a combined treatment of glioblastoma brain tumor or lung cancer with both curcumin and 2-DG. A very important question to ask during this proposed study would be to examine whether the two drugs produce a synergistic, antagonistic, or additive effect in its treatment of cancers. The answer to this question will open various other doors to possible research adventures that could possible lead to an extraordinary discovery. Although a similar research has been done in the past, it did not delve deeply into the mechanistic aspects of it, hence making it a very interesting topic of research.

ACKNOWLEDGMENTS

First of all, I would like to express my sincere gratitude to the Louis Stokes Alliance Minority Participation (LSAMP) program in New York City at the City University of New York (NYC – AMP). Specifically to Dr. Claude Brathwaite and Dr. Francoise Sidime for nominating me for this extraordinary scholarship. Thank you for nominating me among the numerous LSAMP students at the City University of New York (CUNY). I also thank the City College of New York (CCNY – CUNY) for their collaboration with the Austrian Marshall Plan Foundation through whom this research opportunity became a possibility.

Secondly, I am extremely grateful to the Austrian Marshall Plan Scholarship (MPS) foundation for granting me this scholarship. From the list of students that Dr. Brathwaite and Dr. Sidime gave to them, I happened to be one of the very few chosen ones to be awarded this scholarship. I had a wonderful learning and cultural experience during this summer research in Austria and I never had to pay a penny from out of my pocket, all thanks to the Marshall Plan Foundation.

My next appreciation goes to Dr. Juliane Gertrude Bogner-Strauss who accepted to host me in her lab. Not only that, but she took me under her wings and treated me as one of her students. I never felt alone from the very first day I arrived in her lab until the day I left. Her friendly, down-to-earth, and outgoing demeanor made it so much easier to work with her. Her lab cultural activities allowed me to easily associate and work with the students in the lab.

I would also like to say a special thank you to Kathy Walter, the Ph.D. student with whom I worked directly. She willingly shared part of her work with me and guided me through what I needed to know in order to enable me get my work done.

Another special thanks goes to all the members of Dr. Juliane Bogner-Strauss' laboratory – Kathy K, Melina A, Thomas S, Wolfi W, Irene S, Jurgen N, Wenmin X, and Gabriel Z – for making my work in the Bogner-Strauss lab be a pleasant one and for giving me tips on how to have a good stay in Graz and in Austria as a whole.

I am equally grateful to Ms. Katrin Landfahrer for helping provide me with the necessary information to help make my research trip a success.

I cannot conclude without thanking Milestone student housing for the lovely, clean, and well-equipped apartment where I dormed for the duration of my stay in Graz. I will recommend it to anyone.

REFERENCES

Ariyannur, P. S., Moffett, J. R., Madhavarao, C. N., Arun, P., Vishnu, N., Jacobowitz, D., Hallows, W. C., Denu, J. M., Namboodiri, A. M. (2010). Nuclear-cytoplasmic localization of acetyl coenzyme A synthetase-1 in the rat brain. *J Comp Neurol*518:2952–2977.

Cancer Chemother Rep 2 (1972) (3)1:325

Galluzzi L., Bravo-San Pedro J. M., Demaria S., Formenti S. C., & Kroemer G. (2017). *Nat Rev Clin Oncol.* 14(4):247-258. doi: 10.1038/nrclinonc.2016.183. Epub 2016 Nov 15. Review.

Glick, D., Barth, S., & Macleod, K. F. (2010). Autophagy: cellular and molecular mechanisms. *The Journal of Pathology*, *221*(1), 3–12. http://doi.org/10.1002/path.2697

Hoshino, H. and Kubota, M. (2014), Canavan disease: Clinical features and recent advances in research. Pediatr Int, 56: 477–483. doi:10.1111/ped.12422

Korcok, J., Dixon, S. J., Lo T. C., & Wilson, J. X. (2003). Differential effects of glucose on dehydroascorbic acid transport and intracellular ascorbate accumulation in astrocytes and skeletal myocytes. *Brain Res.* 993(1-2):201-7

Langone, P., Debata, P. R., Inigo, J. D. R., Dolai, S., Mukherjee, S., Halat, P., Mastroianni, K., Curcio, G. M., Castellanos, M. R., Raja, K. and Banerjee, P. (2014), Coupling to a glioblastoma-directed antibody potentiates antitumor activity of curcumin. Int. J. Cancer, 135: 710–719. doi:10.1002/ijc.28555

Levine, B. (2007) Cell biology: Autophagy and cancer. Nature 446:745–747.

Levine, B., Klionsky, D. J. (2004) Development by self-digestion: Molecular mechanisms and biological functions of autophagy. Dev. Cell 6:463–477.

Levine, B., & Kroemer, G. (2008). Autophagy in the Pathogenesis of Disease. *Cell*, *132*(1), 27–42. http://doi.org/10.1016/j.cell.2007.12.018

Moffett, J. R., Arun, P., Ariyannur, P. S., & Namboodiri, A. M. A. (2013). *N*-Acetylaspartate reductions in brain injury: impact on post-injury neuroenergetics, lipid synthesis, and

protein acetylation. *Frontiers in Neuroenergetics*, *5*, 11. http://doi.org/10.3389/fnene.2013.00011

Moffett, J. R., Ross, B., Arun, P., Madhavarao, C. N., & Namboodiri, M. A. A. (2007). *N*-Acetylaspartate in the CNS: From Neurodiagnostics to Neurobiology. *Progress in Neurobiology*, *81*(2), 89–131. http://doi.org/10.1016/j.pneurobio.2006.12.003

Mukherjee S., Baidoo J., Fried A., Atwi D., Dolai S., Boockvar J., Symons M., Ruggieri R., Raja K., & Banerjee P. (2016). Curcumin changes the polarity of tumor-associated microglia and eliminates glioblastoma. *Int J Cancer*. Dec 15;139(12):2838-2849. doi: 10.1002/ijc.30398. Epub 2016 Sep 24.

Pessentheiner, A. R., Pelzmann, H. J., Walenta, E., Schweiger, M., Groschner, L. N., Graier, W. F., & Bogner-Strauss, J. G. (2013). NAT8L (*N*-Acetyltransferase 8-Like) Accelerates Lipid Turnover and Increases Energy Expenditure in Brown Adipocytes. *The Journal of Biological Chemistry*, *288*(50), 36040–36051. http://doi.org/10.1074/jbc.M113.491324

Prokesch, A., Pelzmann, H. J., Pessentheiner, A. R., Huber, K., Madreiter-Sokolowski, C. T., Drougard, A., & Bogner-Strauss, J. G. (2016). N-acetylaspartate catabolism determines cytosolic acetyl-CoA levels and histone acetylation in brown adipocytes. *Scientific Reports*, *6*, 23723. http://doi.org/10.1038/srep23723

Seo, M., Crochet, R. B., and Lee, Y.-H., (2014) Chapter 14 - Targeting Altered Metabolism—Emerging Cancer Therapeutic Strategies, In Cancer Drug Design and Discovery (Second Edition), edited by Stephen Neidle, *Academic Press*, San Diego, 427-448, ISBN 9780123965219, https://doi.org/10.1016/B978-0-12-396521-9.00014-0. (https://www.sciencedirect.com/science/article/pii/B9780123965219000140).

Stein, M., Lin, H., Jeyamohan, C., Dvorzhinski, D., Gounder, M., Bray, K., … DiPaola, R. S. (2010). TargetingTumor MetabolismWith 2-Deoxyglucose in Patients With Castrate-Resistant Prostate Cancer and Advanced Malignancies. *The Prostate*, *70*(13), 1388–1394. http://doi.org/10.1002/pros.21172

Sun, L., Yin, Y., Clark, L. H., Sun, W., Sullivan, S. A., Tran, A. Q., … Bae-Jump, V. L. (2017). Dual inhibition of glycolysis and glutaminolysis as a therapeutic strategy in the treatment of ovarian cancer. *Oncotarget*, *8*(38), 63551–63561. http://doi.org/10.18632/oncotarget.18854

Travis, W. D., Brambilla, E., Noguchi, M., … Yankelewitz, D. (2011) International Association for the Study of Lung Cancer/American Thoracic Society/European Respiratory Society international multidisciplinary classification of lung adenocarcinoma. *J Thorac Oncol*. 6:244–285.

U.S. Cancer Statistics Working Group. (2017) *United States Cancer Statistics: 1999–2014 Incidence and Mortality Web-based Report.* Atlanta (GA): Department of Health and Human Services, Centers for Disease Control and Prevention, and National Cancer Institute; 2017.

Vander Heiden, M. G., Cantley, L. C., & Thompson, C. B. (2009). Understanding the Warburg Effect: The Metabolic Requirements of Cell Proliferation. *Science (New York, N.Y.)*, *324*(5930), 1029–1033. http://doi.org/10.1126/science.1160809

Yang, Z., & Klionsky, D. J. (2009). An Overview of the Molecular Mechanism of Autophagy. *Current Topics in Microbiology and Immunology*, *335*, 1–32. http://doi.org/10.1007/978-3-642-00302-8_1

Zand, B., Previs, R. A., Zacharias, N. M., Rupaimoole, R., Mitamura, T., Nagaraja, A. S., & Sood, A. K. (2016). Role of Increased n-acetylaspartate Levels in Cancer. *JNCI Journal of the National Cancer Institute*, *108*(6), djv426. http://doi.org/10.1093/jnci/djv426

Zanotto-Filho, A., Braganhol, E., Klafke, K., Figueir, F., Terra, S. R., Paludo, F. J., Morrone, M., Bristot, I. J., Battastini, A. M., Forcelini, C. F., Bishop, A. J. R., Gelain, D. P., & Moreira, J. C. F. (2014). Autophagy inhibition improves the efficacy of curcumin/temozolomide combination therapy in glioblastomas. *Cancer Letters*, 358 (2): 220 – 231

Zhao, Q., Chu, Z., Zhu, L., Yang, T., Wang, P., Liu, F., … Zhao, Y. (2017). 2-Deoxy-d-Glucose Treatment Decreases Anti-inflammatory M2 Macrophage Polarization in Mice with

Tumor and Allergic Airway Inflammation. *Frontiers in Immunology*, *8*, 637. http://doi.org/10.3389/fimmu.2017.00637

Zhu, Y., & Bu, S. (2017). Curcumin Induces Autophagy, Apoptosis, and Cell Cycle Arrest in Human Pancreatic Cancer Cells. *Evidence-Based Complementary and Alternative Medicine : eCAM*, *2017*, 5787218. http://doi.org/10.1155/2017/5787218